A Mean Field Game-Theoretic Cross-Layer Optimization for Multi-Hop Swarm UAV Communications

Tong Li, Cong Li, Chungang Yang, Junqi Shao, Yue Zhang, Lei Pang, Lizhong Chang, Lingli Yang, and Zhu Han

***Abstract*—Unmanned aerial vehicle (UAV) multi-hop communication networks are foreseen to be widely employed in both military and civilian scenarios. However, in ultra-dense scenarios with swarm UAVs, nodes are highly dynamic mobile, ultra-dense deployment and non-centralized distribution. These characteristics make the centralized resource management policy not apply. Meanwhile, existing routing protocols can't meet the performance challenges of high dynamic, topology and link frequency changes of ultra-dense scenarios with swarm UAVs. To solve the above challenges of resource management and routing protocol, a cross-layer optimization method is presented with a novel mean field game (MFG) in this paper. It is based on the cross-layer design method of the MFG theory and jointly considers the power resources in the physical layer, frequency resources in the medium access control (MAC) layer, and routing resources in the network layer. By dividing into subproblems, the original problem is solved. Meanwhile, the optimal data transmission path can be selected through the management and allocation of frequency resources and power resources. A cross-layer resource management dynamic source routing (CLRM-DSR) protocol is designed based on that which adds link quality measurement. The simulation results show that the presented CLRM-DSR with the proposed resource management scheme can improve the data packet transmission rate, reduce end-to-end delay, and lower routing overhead for the multi-hop swarm UAV communication network.**

***Index Terms*—Cross-layer optimization, MFG, multi-hop communications, UAV**

Manuscript received March 29, 2021; revised August 9, 2021; approved for publication by Hyoil Kim, Division III Editor, September 27, 2021.

This work was supported in part by the CETC Key Laboratory of Data Link Technology (CLDL-20182308 and CLDL-20202314), and by the Aeronautical Science Foundation of China (ASFC-2018ZG81002). This work is also partially supported by US NSF CNS-2128368, CNS-2107216, Toyota and Amazon. The authors Tong Li and Chungang Yang are also with the CETC Key Laboratory of Data Link Technology. We built the multi-hop UAV communication platform for the past four years. Corresponding author Chungang Yang thanks for current and previous members of GUIDE family including Tong Li (2020), Junqi Shao, Lizhong Chang and Lei Pang (2018), Lingli Yang (2019), Yue Zhang (2017) for their cooperation on the platform. Meanwhile, here we thanks to co-authors Dr. Cong Li and Prof. Zhu Han for their contributions, meaningful discussion, and valuable guidance on the platform and this work.

T. Li, C. Yang, J. Shao, Y. Zhang, L. Pang, L. Chang, and L. Yang are with the State Key Laboratory on Integrated Services Networks, Xidian University, Xi'an, 710071 China, email: {15339118964, chgyang2010, ruya0905, yuez_0907, panglei722}@163.com, lzchang.66@foxmail.com, yll99887788@163.com.

C. Li is with the Academy of Space Electronic Information Technology, Xi'an, 710100, China, email: lic1@cast504.com.

Z. Han is with the Department of Electrical and Computer Engineering in the University of Houston, Houston, TX 77004 USA, and also with the Department of Computer Science and Engineering, Kyung Hee University, Seoul, South Korea, 446-701, email: hanzhu22@gmail.com.

Digital Object Identifier: 10.23919/JCN.2021.000035

I. INTRODUCTION

DUE to the flexibility, easy deployment, relatively low cost, wide coverage, and massive connectivity of unmanned aerial vehicles (UAVs) [1], [2], UAV communications have attracted increasing research attention and applications. UAV systems have been used to take many tasks, such as Internet of things (IoT) data transmission [1], border surveillance [3], disaster monitoring [4], and emergency communications [5]. At present, tasks are getting more complex, and a single UAV faces different challenges such as limited power, short-communication ranges, rapid topology, low bandwidth, and handover [6]. Therefore, the applications of UAVs become networking and clustering, and flying ad-hoc network (FANET) has been widely investigated [7].

Benefiting from the centerless, self-organizing, and multi-hop communication, FANET meets the requirements of multi-node collaboration for complex tasks [8]. However, FANET also faces many challenges in practical applications:

- *Resource management*: FANET is a network that is limited by energy and bandwidth, where the dynamicity of UAVs may lead the network to be reconfigured frequently [8]. This may lead to network instability for the conventional centralized resource management schemes, which are also low efficient and lack scalability.
- *Routing protocol*: In FANET, the performance of routing protocol determines the stability, accuracy and timeliness of data transmission. Applications to FANET have different requirements for UAV speeds, and the link is with a high bit error rate (BER) due to the interference [9]. Additionally, the requirements of reliability from the FANET are also diverse. To meet the requirements of FANET, such as reliable services, multi-service transmission, low latency, and efficient routing, the routing protocol needs to satisfy the unique features especially with ultra-dense, dynamic topology, and diverse services. Designing a reliable routing protocol for the FANET becomes another challenge.

This paper focuses on the swarm FANET, mainly discusses the application of the cross-layer design method and mean field game (MFG) theory to optimize the routing protocol in the large-scale FANET. In the traditional hierarchical model, the limitation of communication is broken by the cross-layer design method. All layers can share local information through cross-layer interaction, which can effectively improve the utilization of the resource of FANET. It is clear that for analyzing, modeling, and solving power control of large-scale networks. The MFG theory provides a feasible method. A cross-layer resource management method is proposed, considering the power resources of the physical layer, the frequency resources of the medium access control (MAC) layer, and the routing resources of the network layer. According to the characteristics of FANET, the dynamic source routing (DSR) protocol is focused on. Furthermore, we add the link quality measurement to improve the DSR protocol.

We list our main contributions of our paper below:

- *Cross-layer resource management algorithm using MFG*: In this paper, for the conventional centralized resource management schemes that are low efficient in swarm UAV networks with limited resources, the resource management algorithm is proposed, which combines the physical layer, MAC layer, and network layer. The cross-layer design can effectively improve the resource utilization and MFG can take into account both local and entire network resource utilization of FANET. Through the management and allocation of power resources and frequency resources in the physical layer and MAC layer using MFG, we design the cross-layer optimization cost function to maximize the energy utilization efficiency.
- *Cross-layer resource management dynamic source routing (CLRM-DSR) protocol in FANET*: Aiming at the rapid change of the network topology caused by high dynamic characteristics of FANET, we have added the link quality into DSR to provide the optimal solution for network routing. In the CLRM-DSR protocol, the link quality combines with the cross-layer cost function, which can be obtained by the cross-layer resource management algorithm. By comparing the link quality, the data transmission path in the network layer is planned, and the network performance of information transmission is improved.
- *FANET simulation platform*: A FANET simulation platform is built, which is used to construct a discrete-time simulation environment for the CLRM-DSR and the proposed cross-layer resource management algorithm. It integrates the physical layer, MAC layer and network routing implementation. Meanwhile, this simulation platform can also implement the algorithm verification of the conventional mobile ad-hoc network (MANET), the vehicle ad-hoc network (VANET).

The rest of this paper is structured as follows. Section II summarizes the research status about the cross-layer design, MFG and routing protocols. Section III models the swarm FANET system and cross-layer resource management problem. In Section IV, how to obtain the cross-layer resource management algorithm by decomposing that problem into subproblems and solving them is described. Meanwhile, how to apply these algorithms in the DSR protocol is explained. Section V introduces the FANET simulation platform and analyzes the performance improvement of the cross-layer resource management algorithm in the ultra-dense scenario. Finally, the conclusion and future work are drawn in Section VI. Table I lists the acronyms that appear in this paper.

TABLE I
ACRONYMS AND FULL SPELLING.

Acronym	Full spelling
UAV	Unmanned aerial vehicle
MFG	Mean field game
MAC	Medium access control
CLRM-DSR	Cross-layer resource management dynamic source routing
IOT	Internet of things
FANET	Flying ad-hoc network
BER	Bit error rate
DSR	Dynamic source routing
MANET	Mobile ad-hoc network
VANET	Vehicle ad-hoc network
D2D	Device-to-device
BS	Base station
ACO	Ant colony optimization
AODV	Ad-hoc on-demand distance vector routing
TBRPF	Topology broadcast based on reverse-path forwarding
HJB	Hamilton-Jacobi-Bellman
FPK	Fokker-Planck-Kolmogorov
MFE	Mean field equilibrium

II. RELATED WORKS

Typically, network resource management has been widely studied, which is always described as a constrained optimization problem with a specific utility function or cost function [10]. The FANET resource management problem involves more complex aspects: rate allocation, bandwidth allocation, power control, frequency scheduling, access control, topology management, routing, or end-to-end quality of service [11]. It aims to allocate network resources dynamically, improve network performance, maximize network utility and provide end-to-end quality of service under the conditions of low latency, time-varying channel, finite bandwidth, and dynamic topology [12].

One of the tools for designing resource management algorithms is the cross-layer design [13]. It breaks the communication restriction between layers, which is different from the modular layered design method [14]. In this way, the network divided into multiple layers can be designed, analyzed, optimized, and controlled as a whole. As described in [15], the cross-layer framework created for routing, relay selection, and power allocation is capable of improving user utility and reducing power loss. In [16], the cross-layer design method was adopted for real-time video transmission. When the data need to be transmitted, the payload will be passed from the transport layer to the network layer and the MAC layer, while the capacity information will be fed back from the MAC layer to the other layers. By combining multiple protocol layers, [17] implemented cross-layer modeling and optimization of multi-dimensional resources. However, the cross-layer design method used in FANET lacks a unified cross-layer optimization goal, and the dynamic relationship between the layers remains unclear [18]. Therefore, we need an approach that can take into account the multi-dimensional cross-layer resource model, interaction mechanism, and spatio-temporal dynamic relationship of resources.

Currently, many game models for multi-hop networks are presented [19] and researchers have applied game theory to the resource management of the FANET [20]–[22]. Game theory has some advantages over other conventional methods. Firstly, it can solve different problems with multiple players. During the game, multiple different goals on a player can be jointly optimized, and the rational behavior characteristics of multiple participants can be described. Secondly, it can model the interaction between players, analyze equilibrium and provide insights to design distributed resource management algorithm [1].

Authors in [23] presented a survey of using game theoretic techniques to deal with the problems in UAV wireless communication networks and those game theories are compared. Conventional game theory has complex information interaction and high communication overhead when applied to swarm FANETs. Meanwhile, it takes a longer time to reach equalization with the increasing number of UAVs [1]. Fortunately, MFG is an effective method to solve UAV resource management in such ultra-dense networks due to the following reasons:

- *Less information interaction complexity*: Game theory can maximize the utilization of resources in the local and entire network, and improve the utilization of network resources while ensuring user fairness and service quality. They are used to optimize the spectrum efficiency of the local and whole network. However, unlike conventional game theory, MFG can model and analyze the interaction between individual behavior and collective behavior of a swarm FANET. Instead of modeling the interaction process between players, MFG models individual behavior through group actions, which minimizes the complexity of information interaction.
- *Low communication overhead*: By definition, MFG has state space, action space and policy control. The player's policy control can map a state in the state space to action in the action space for a pre-defined period time in MFG. As a result, the players' information that needs to exchange among different UAVs in the FANET is low, and the communication overhead generated by information exchange is less than the applications of other game theories. MFG theory processes the influence of all nodes by using mean field theory (MFT), and replaces the sum of a single effect with an average effect, which simplifies the analysis process and reduces the calculation amount of the game solution.
- *Adaptability of ultra-dense scenario*: As the number of nodes increases, the value of the mean field in MFG is more able to characterize the real environmental value. While the number of nodes tends to infinity, the MFG equilibrium approaches the Nash equilibrium or the Markov equilibrium. MFG is a special type of stochastic differential game, which is mainly used for the modeling of large-scale systems dynamic analysis.

For the advantages of MFG, the MFG has been proposed for power control in different types of cellular networks. The author in [24] designed an interference-aware and power control scheme based on MFG to improve energy and spectrum efficiency in a 5G ultra-dense cellular network. In [25], MFG is adopted to divide complex large-scale optimization problems into a series of local optimization problems, significantly reducing the communication overhead and convergence time of interference management in the heterogeneous network. Thus, each small cell base station can implement its policy by using only its local information and some macroscopic information. Authors in [26] presented a distributed control and energy-aware power control algorithm for ultra-dense device-to-device communication (D2D) networks based on MFG theory. The control problem considers both the energy remaining in the device batteries and the interference caused by the communication devices to others. Authors in [27] proposed a downlink power control algorithm in ultra-dense cellular networks where base stations (BSs) are uniformly distributed over a two-dimensional infinite Euclidean plane. In this model, users are distributed independently of BSs, and the BSs with no user within the coverage stay dormant to serve energy.

TABLE II
APPLICABILITY OF PROTOCOLS TO UAV NETWORK.

Protocol type	Problems in application to UAV network
Static	Fixed tables, not suitable for dynamic topology, does not handle changes well, not scalable, higher possibility of human errors [3]
Proactive	Large overhead for maintaining tables up-to-date, bandwidth constrained networks cannot use them, slow reaction to topology changes results in delays, not suitable for large network topologies [3], [42]
OLSR	Higher overheads, routing loops, slow to reacting of failures [42], [43]
DSDV	Consumes large network bandwidth, higher overheads, periodic updates [44], [45]
Reactive	High latency in route finding, source routing does not scale well, for large network overhead may increase because of large header size table [3], [42]
DSR	Lower route overhead at the cost of delays during route construction [46], [41]
AODV	Link failure may trigger route discovery more delays and higher bandwidth as the size of the network increases [44], [41]
Hybrid	Complex cluster head selection algorithm, difficult to be used in dynamic network [3]
Geographic 3D	Requires location information which may become unrealistic in many applications [3]

Despite numerous research conducted in this field, most schemes have focused on terrestrial networks. Different game-theoretic techniques and their applications have different wireless communication and networking problems in specific communication networks [28]. In swarm FANET, due to the limitation of node capacity, the resources management using MFG needs to solve multiple problems, such as the power control, the frequency scheduling and the interference problem.

FANET appears as an extension of VANET or MANET at the beginning, which can work in areas that VANET or MANET cannot reach [29]. In the related researches and experiments of the FANET, the routing protocol required for networking uses the existing MANET routing protocol [30], [31]. The author in [32] focused on the enhancement of the opti-

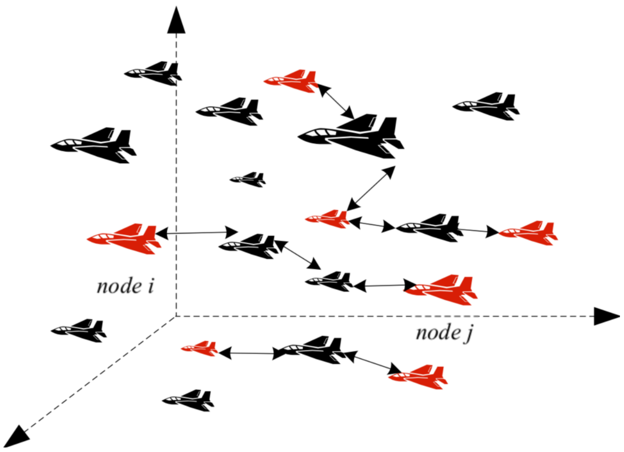

Fig. 1. A swarm scenario of FANET.

mized link-state routing (OLSR) protocol in FANET specifically on node-link expiration and residual energy. Authors in [33] proposed the solution that counts the link quality information directly using the physical layer to optimize the routing. [34] presented a novel routing protocol for FANET using modified AntHocNet, which is better than generic ant colony optimization (ACO) and other traditional routing protocols utilized in FANET. [35] enhanced the FANET network packet delivery rate by reducing unnecessary rebroadcast messages in ad-hoc on-demand distance vector routing (AODV) protocol. [36] designed the adaptive HELLO message interval in routing protocol to improve the energy utilization efficiency of the nodes in FANET, which makes the routing protocol meets the network performance requirements with the lowest energy cost. Stanford research institute (SRI) International conducted the first flight experiment of the FANET [37]. Topology broadcast based on reverse-path forwarding (TBRPF) is used as the network layer routing protocol, and TBRPF is a proactive routing protocol, which effectively reduces the routing overhead [38]. Authors in [39] designed another FANET test platform using the dynamic source routing (DSR) protocol. Khare believes that the DSR protocol only initiates the route lookup process when the source nodes have data transmission, which is more effective for the high mobility of the node and the dynamic change of the topology of the FANET than the proactive routing protocol [40]. In another recent study in [41], the authors concluded that DSR has the highest throughput and is the most suitable routing protocol among others in a high movement and dynamic network. Table II summarizes the routing protocols in MANET and their applicability to the UAV environment.

III. System Model and Problem Model

A. System Model

A swarm FANET scenario is shown in Fig. 1. In this paper, this FANET scenario can be described by using a directed graph. There is a pair of the source node (node *i*)-destination node (node *j*) on this scenario, and some mathematical symbols are listed as follows:

- $\mathcal{G} = (\mathcal{V}, E)$, considering asymmetric links in the FANET, the topology is defined as a directed graph, where $\mathcal{V} = \{1, 2, \cdots, M\}$ is the set of UAVs and E is the wireless links for communication between nodes.
- $\mathcal{A}^{\mathcal{G}} = \{a_{ij}\}_{i,j\in V}$, when $(i, j) \in E$, $a_{ij} = 1$, it means that node *i* can directly communicate with node *j*.
- $\mathcal{V} = S \cup R \cup D$, assuming that the FANET system is composed of a series of transmitting nodes, receiving nodes, and relay nodes, where $\mathcal{S}$ is the transmitting node set, $\mathcal{R}$ is the receiving node set, and $\mathcal{D}$ is the relay node set.
- $\mathcal{F} = \{f_{\min}, f_{\min+1}, \cdots, f_{\max-1}, f_{\max}\}$, which is the available radio spectrum resources in the FANET. Meanwhile, the bandwidth between adjacent spectrum can be defined as w.
- $E^{\max}$, the available maximum energy for UAV.
- $\mathcal{Q}(t) = \{q_1, \cdots, q_M\}$, the set of packet queue length on UAVs at time *t*.
- $\mathcal{X} = \{x_1, \cdots, x_M\}$, the set of UAV geographical location. Each element is composed of longitude, latitude, and height.

The corresponding UAV energy model, information queue model, and mobility model are defined as the sequel.

The *energy model* of UAV is defined as

$$E_{j,t+1} = E_{j,t} - \delta \cdot p_{j,t}, \tag{1}$$

where $p_{j,t}$ is the power of node j at time t. δ is the step in the time dimension, and its value depends on the designed algorithm.

The *information queue model* of UAV is

$$q_{j,t+1} = [q_{j,t} - D_j 1_{\text{success}}(t, s)]_+ + A_{j,t+1}, \tag{2}$$

where $D_j 1_{\text{success}}(t, s)$ is the process of transmitting a packet from the queue on the UAV, $A_{j,t+1}$ is the process of adding packets to the queue on the UAV.

The *mobility model* is defined as

$$x_{j,t+1} = x_{j,t} + \delta \cdot v(t, x_{j,t}) + \sigma_x w_{j,t+1}, \tag{3}$$

where $w_{j,t+1}$ is a Wiener process with a mean of zero and a limited variance. δ_x is a value greater than zero. $v(t, x_{j,t})$ is a function related to the speed of UAVs.

Establishing an appropriate *interference model* can improve the overall performance and resource utilization of a wireless network [47]. In the FANET, the interference interaction model is considered as follows. Assuming that nodes i and j are communicating at frequency f, the transmission of node j's neighbor node k at frequency f will interfere the node j. Since the signal is transmitted over the wireless link, the path loss model and channel fading model are considered as (4) and (5).

The *path loss model* is

$$l_{i,j}^f = \min\left(1, \|z_i - z_j\|^{-\alpha(f)}\right), \tag{4}$$

where $\alpha(f) > 2$ is the path loss index, z_j is the location of node j, and $\|z_i - z_j\|$ is the Euclidean distance between nodes i and j.

The *channel fading dynamic model* is [48]

$$dg_{i,j}^f(t) = \frac{1}{2}\left(\mu^f - g_{i,j}^f(t)\right)dt + \eta^f dW_{i,j}^f(t), \tag{5}$$

where μ^f is a non-negative constant, η^f is greater than zero but less than infinity, and $W_{i,j}{}^f(t)$ is a mutually independent Wiener process.

Based on path loss model and channel fading model, the channel gain of link (i,j) is defined as

$$\left|h_{i,j}^f(t)\right|^2 = l_{i,j}^f \times \left|g_{i,j}^f(t)\right|^2. \quad (6)$$

Therefore, the interference of the link (k,j) at frequency f and time t to link (i,j) is

$$I_j^f(t) = \sum_{\substack{k\in V\\ k\neq i}} p_k^f(t)\left|h_{k,j}^f(t)\right|^2. \quad (7)$$

B. Problem Model

In order to reduce inter-link interference and maximize energy utilization, the problem of cross-layer resource management can be constructed as a stochastic game model, which is defined as $M = (\mathcal{N}, \mathcal{X}, \mathcal{A}, \mathcal{T})$:

- $\mathcal{N}$: The set of players, $\mathcal{N} = \{1, 2, \cdots, N\}$, where N represents the number of players in the game. It is defined as $\mathcal{N} = S$, which refers to the set of transmitting nodes.
- $\mathcal{A}$: Action set of players, including UAV power selection, spectrum allocation, and next-hop node selection.
- $\mathcal{T}$: The cost function combining with physical layer power resources, MAC layer frequency resources, and network layer routing resources.

In order to maximize the utilization of local and entire network resources without significantly increasing routing overhead, the cost function on link (i,j) is defined as

$$T_{i,j}^f(t) = \frac{1}{c_{i,j}^f(t)\cdot\left[Q_i(t) - Q_j(t)\right]^+ e^{-v_{i,j}^t\beta}}, \quad (8)$$

$$c_{i,j}^f(t) = \frac{w\cdot\log_2\left[1+\gamma^j\right]}{p_i(f)}, \quad (9)$$

$$\gamma^j = \frac{p_i(f)\left|h_{i,j}^f(t)\right|^2}{N_j(f) + I_j^f(t)}. \quad (10)$$

where $c_{i,j}^f(t)$ is the energy efficiency on link (i,j), the higher the efficiency of the energy on the link, the smaller the loss on the link, which is more suitable for data transmission than other links.$N_i(f)$ is background noise. $Q_i(t)$ and $Q_j(t)$ are the length of packet queue at nodes i and j, respectively. The greater the difference between the packet queues on node i and node j, the more stable the link, otherwise it will not be selected for data transmission. $v_{i,j}^t$ is the relative speed of nodes i and j at time t. The smaller the relative speed between nodes, the more stable the link for data transmission. In general, the smaller the value of the cost function, the more stable the link and the more suitable the link for data transmission.

Supposing that K_i is the number of relays passed by player S_i in the transmission path, and the cost of player S_i can be defined as

$$T_i = \sum_{j=0}^{K_i+1} T_{j,j+1}^f, \quad (11)$$

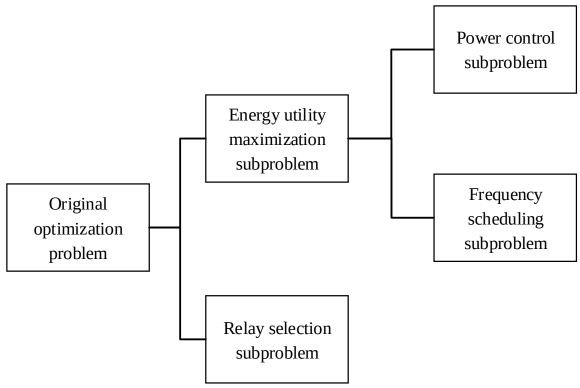

Fig. 2. Decomposition of the original optimization problem.

where $j=0$ and $j=K_i+1$ represent player j itself and the receiving node corresponding to player j, respectively. When the distance from node j to the receiving node $j+1$ is closer than other receiving nodes, node $j+1$ is a feasible next hop node for node j. And the set of feasible next hop nodes of node j is defined as $next(j)$.

Then the cross-layer resource management problem can be described as

$$\min T_i = \sum_{j=0}^{K_i+1} T_{j,j+1}^f \quad (12a)$$

$$s.t. \quad f\in F, \quad (12b)$$

$$0 < p \le p^{\max}, \quad (12c)$$

$$j+1 \in next(j), \quad (12d)$$

$$\gamma^j \ge \gamma^{th}, \quad (12e)$$

where objective function (12a) is to minimize the cost of node i. The first condition (12b) constrains the frequency of UAV communication. The second constraint (12c) takes into account the limited transmitting power of UAVs. Whereas the third constraint (12d) means that node $j+1$ is in the set of j's next hop, and node j can communicate with it in one hop. The last constraint (12e) indicates that the packet can be received correctly only if the signal to interference plus noise ratio (SINR) at the receiving node j is greater than the threshold value γ^{th}.

IV. Solution to the Cross-Layer Resource Management Problem

The cross-layer cost function in (8) and cross-layer resource management problem in (12) are shown in the previous section. However, it is difficult to solve them directly because of the complexity of the original optimization problem [49]. Meanwhile, the UAV resource management and the choice of the path are relatively independent in origin problem (12). Thus, it can be decomposed into the link energy utility maximization subproblem and relay selection subproblem.

Power and frequency are two variables that need to be optimized in the energy utility maximization subproblem. Frequency scheduling is a fast process that executes at the beginning of a time slot ranging from time 0 to time t. In contrast, power control is a slow process. Since frequency scheduling and power control are two separate processes, the energy utility maximization subproblem can be further decomposed into a power control subproblem and a frequency scheduling subproblem. Fig. 2 shows the decomposition of the original problem. The brief solutions to these subproblems are as follows:

1) *Energy utility maximization subproblem*: This problem can be solved by power control and frequency scheduling algorithms under the condition of a given link (i, j).
2) *Power control subproblem*: Given the frequency $f \in F$, the power control algorithm is designed by MFG theory.
3) *Frequency scheduling subproblem*: The optimal frequency scheduling scheme, $f^* = \arg\max c_{i,j}^f$, can be obtained by the power control algorithm under the condition of any frequency $f \in F$.
4) *Relay selection subproblem*: It can be transformed into a problem that maximizes $[Q_i(t) - Q_j(t)]^+ e^{-v_{i,j}^t \beta}$. Any node $j \in next(i)$ can get the optimal relay node j^* by executing the energy utility maximization algorithm and calculating $\arg\min T_{i,j}$.

In summary, the power control algorithm based on MFG theory is the basis of the cross-layer resource management algorithm. Therefore, this paper will introduce the solution to the power control subproblem in detail in the next subsection.

A. Power Control Solution

In the MFG model of power control, the players are a set of sending nodes. The action space includes all feasible power resources. The state space is defined as the node energy state space and the interference state space of the node. The utility function is as (11).

Firstly, the value function is defined as

$$u_{i,j}(t) = \max E\left[\int_t^T c_{i,j}^f(\tau)\, d\tau + c_{i,j}^f(T)\right], t \in [0, T], \tag{13}$$

where $c_{i,j}^f(T)$ is the utility function at the final time T. According to the Bellman optimality principle, an optimal control strategy should be satisfied: the remaining decision must constitute the optimal strategy for the state of the previous decision-making regardless of the state and decision of the past.

For any link (i, j), the optimal power scheme $p_i^*(t \to T)$ can make equation in (14) true at any time $t \in (0, T)$.

$$E\left[\int_t^T c_{i,j}^f(p_i^*(\tau))\, d\tau + c_{i,j}^f(T)\right] = u_{i,j}(t), t \in [0, T] \tag{14}$$

Secondly, the mean field function is defined as

$$m(t, x) = \lim_{N \to \infty} \frac{1}{N} \sum_{i=1}^{N} I_{\{x(t) = x\}}, \tag{15}$$

where N is the number of players, which is huge and even goes to infinity. I is a Boolean indicator function. $x = (e, \mu)$ is the system state of MFG, where e and μ are energy state and interference state, respectively.

According to MFG theory, the MFG system consists of Hamilton-Jacobi-Bellman (HJB) equation and Fokker-Planck-Kolmogorov (FPK) equation. The value function satisfies the HJB equation and the mean field function satisfies the FPK equation. The MFG equilibrium solution can be obtained by solving related equations.

The HJB equation and the FPK equation of the MFG system are further derived. Assuming that dt is an infinitesimal amount of time, (16) at time $t \to t + dt$ can be obtained according to Bellman's optimality principle.

$$u(t_0, x_0) = \min_p \left\{ \begin{array}{l} \mathrm{E}u(t_0 + dt, x_0 + dx + \sigma dB_t) \\ +c(t_0, x_0)\, dt \end{array} \right\}, \tag{16}$$

where $\sigma = (0, \sigma_\mu)$ and $B_t = (0, {B_t}^\mu)$.

(17) can be obtained by expanding in (16) through the Taylor formula and Ito's rule.

$$\begin{aligned} &u(t_0 + dt, x_0 + dx + \sigma dB_t) \\ =&u(t_0, x_0) + \partial_t u(t_0, x_0)\, dt + \nabla_e u(t_0, x_0)\, de \\ &+ \nabla_\mu u(t_0, x_0)(d\mu + \sigma_\mu dB_t^\mu) + \frac{1}{2}\sigma_\mu^2 \frac{\partial^2 u(t_0, x_0)}{\partial \mu^2} dt + o, \end{aligned} \tag{17}$$

where $de = -p(t_0, x_0)\, dt$ and $d\mu = \nabla_t \mu(t_0, x_0)\, dt$. When the higher order infinity is ignored, (18) can be obtained by taking the expectation of both sides of (17),

$$\begin{aligned} &Eu(t_0 + dt, x_0 + dx + \sigma dB_t) \\ &=u(t_0, x_0) + \partial_t u(t_0, x_0)\, dt \\ &\quad + \nabla_e u(t_0, x_0)\, de \\ &\quad + \nabla_\mu u(t_0, x_0)\, d\mu \\ &\quad + E[\nabla_\mu u(t_0, x_0)\, \sigma_\mu dB_t^\mu] \\ &\quad + \frac{1}{2}\sigma_\mu^2 \Delta_\mu u(t_0, x_0)\, dt. \end{aligned} \tag{18}$$

Since the expectation of Brownian motion dB_t^μ is zero at time dt, (18) can be simplified into (19),

$$\begin{aligned} &Eu(t_0 + dt, x_0 + dx + \sigma dB_t) \\ &=u(t_0, x_0) \\ &\quad + \partial_t u(t_0, x_0)\, dt \\ &\quad + \nabla_e u(t_0, x_0)\, de \\ &\quad + \nabla_\mu u(t_0, x_0)\, d\mu \\ &\quad + \frac{1}{2}\sigma_\mu^2 \Delta_\mu u(t_0, x_0)\, dt, \end{aligned} \tag{19}$$

where $\Delta_\mu u(t_0, x_0) = \frac{\partial^2 u(t_0, x_0)}{\partial \mu^2}$. Thus, (20) can be arranged as

$$u(t_0, x_0) = \min_p \left\{ \begin{array}{l} u(t_0, x_0) + \partial_t u(t_0, x_0)\, dt \\ -\nabla_e u(t_0, x_0)\, p(t_0, x_0)\, dt \\ +\nabla_\mu u(t_0, x_0)\, \partial_t \mu(t_0, x_0)\, dt \\ +\frac{1}{2}\sigma_\mu^2 \Delta_\mu u(t_0, x_0)\, dt \\ +c(t_0, x_0)\, dt \end{array} \right\}. \tag{20}$$

The following (21) can be obtained by sorting (20).

$$\begin{aligned}&\partial_t u(t_0,x_0)+\tfrac{1}{2}\sigma_\mu^2\Delta_\mu u(t_0,x_0)\\&=-\min_p\left\{\begin{array}{l}c(t_0,x_0)\\-p(t_0,x_0)\nabla_e u(t_0,x_0)\\+\nabla_\mu u(t_0,x_0)\partial_t\mu(t_0,x_0)\end{array}\right\}\end{aligned}\tag{21}$$

The general form of the HJB equation can be expressed as

$$\begin{aligned}&\partial_t u(t,x)+\tfrac{1}{2}\sigma_\mu^2\Delta_\mu u(t,x)\\&=-\min_{p(t)}\left\{\begin{array}{l}c(t,x)\\-p(t,x)\nabla_e u(t,x)\\+\partial_t\mu(t,x)\nabla_\mu u(t,x)\end{array}\right\}\\&=H(c,p,\nabla_x u(t,x)),\end{aligned}\tag{22}$$

where $H(c,p,\nabla_x u(t,x))$ is the Hamiltonian term.

The FPK equation can be derived by using the test function method. The detailed steps can be referenced in [50]. The derived FPK is

$$\begin{aligned}&\partial_t m(t,x)+\nabla(a(x,\alpha)\cdot m(t,x))\\&-\nabla(p(t,x)\cdot m(t,x))-\frac{\sigma^2}{2}\Delta m(t,x)=0.\end{aligned}\tag{23}$$

The HJB equation in (22) and the FPK equation in (23) have been deduced. Next, the mean field equilibrium (MFE) needs to be achieved. If the objective function of the optimal control problem is convex, the convergence point is MFE. When solving MFE, the finite difference method can be used. This method essentially achieves MFE through iterative steps.

The iteration step size in terms of time, energy and interference is defined as

$$\delta_t=\frac{T}{X},\delta_e=\frac{E^{\max}}{Y},\delta_\mu=\frac{I^{\max}}{Z}.\tag{24}$$

By discretizing the time axis $[0,T]$, energy state space $[0,E^{\max}]$, interference state space $[0,I^{\max}]$ in space $X\times Y\times Z$, and iterating the MFG system equation according to the iteration step size, the MFE can be solved.

In this paper, the Lax-Friedrichs method is used to solve the FPK equation [50]. In this method, the following conditions are assumed: $f(t,x)=f_i^j$, where $t=j\delta_t$, and $x=i\delta_x$. The operator of Lax-Friedrichs can be achieved as

$$\partial_t f_i^j=\frac{f_i^{j+1}-\frac{1}{2}\left(f_{i+1}^j-f_{i-1}^j\right)}{\delta_t},\tag{25}$$

$$\partial_x f_i^j=\frac{f_{i+1}^j-f_{i-1}^j}{2\delta_x},\tag{26}$$

$$\Delta_x f_i^j=\nabla_x\left(\nabla_x f_i^j\right)=\frac{f_{i+2}^j-2f_i^j+f_{i-2}^j}{4\delta_x^2}.\tag{27}$$

The mean field iteration in (28) can be obtained by substituting the above operator into the FPK equation as

TABLE III
SYMBOLS AND NOTATIONS USED IN DERIVATION.

Symbols	Definitions
B_t	Brownian motion
σ	Partial derivative operator
σ^2	Second-order Partial derivative operator
∇	Gradient operator
o	Infinitesimal of higher order
$E[\cdot]$	Mathematical expectation
$\triangle$	Laplace operator
$H(c,p,\nabla_x u(t,x))$	Hamilton term
δ_t	Iteration step size of time
δ_e	Iteration step size of energy
δ_u	Iteration step size of interference
m	The mean field
λ	Lagrange multiplier
L	Lagrange function
L_d	Discrete lagrange function

$$\begin{aligned}\frac{m_{i,j}^{t+1}}{\delta_t}=&\frac{m_{i+1,j+1}^t+m_{i-1,j-1}^t}{2\delta_t}\\&+p(t,x)\frac{m_{i+1,j}^t-m_{i-1,j}^t}{2\delta_e}\\&-a(x,\alpha)\frac{m_{i,j+1}^t-m_{i,j-1}^t}{2\delta_\mu}\\&+\frac{\sigma^2}{2}\frac{m_{i+2,j}^t-2m_{i,j}^t+m_{i-2,j}^t}{4\delta_e^2}.\end{aligned}\tag{28}$$

Due to the existence of the Hamilton term, the finite difference algorithm cannot be used to solve the HJB equation directly. Therefore, the HJB equation is reconstructed to its corresponding optimal control problem, the newly defined problem is

$$\begin{aligned}&\max_{p_i}E\left[\int_0^T c_{i,j}^f(t,x,p,m)d\tau+c_{i,j}^f(T)\right]\\&s.t.\ \partial_t m(t,x)+\nabla(a(x,\alpha)\cdot m(t,x))\\&-\nabla(p(t,x)\cdot m(t,x))-\frac{\sigma^2}{2}\Delta m(t,x)=0.\end{aligned}\tag{29}$$

The Lagrangian function corresponding to the new problem is obtained by introducing a Lagrangian multiplier.

$$\begin{aligned}&(t,x,p,m,\lambda)=\\&\int_{t=0}^T\int_{e=0}^E\int_{\mu=0}^{\mu^{\max}}\left\{\begin{array}{l}c(t,x,p,m)m(t,x)+\\\lambda\left[\begin{array}{l}\partial_t m(t,x)\\+\nabla(a(x,\alpha)\cdot m(t,x))\\-\nabla(p(t,x)\cdot m(t,x))\\-\frac{\sigma^2}{2}\Delta m(t,x)=0\end{array}\right]\end{array}\right\}dtded\mu\end{aligned}\tag{30}$$

After discretizing (30), the Lagrangian multiplier iteration in (31) is obtained by finding the solution $\frac{\partial L_d}{\partial m_{i,j}^t}=0$,

$$\begin{aligned}\frac{\lambda_{i,j}^{t-1}}{\delta_t} =& \frac{\left(\lambda^t_{i+1,j+1}+\lambda^t_{i-1,j-1}\right)}{2\delta_t} \\ &+ \frac{p^t_{i-1,j}\lambda^t_{i-1,j} - p^t_{i+1,j}\lambda^t_{i+1,j}}{2\delta_e} \\ &- \frac{a^t_{i,j-1}\lambda^t_{i,j-1} - a^t_{i,j+1}\lambda^t_{i,j+1}}{2\delta_\mu} \\ &+ \frac{\sigma^2}{2}\frac{\lambda^t_{i-2,j}-2\lambda^t_{i,j}+\lambda^t_{i+2,j}}{4\delta_e^2} - c^t_{i,j}.\end{aligned} \tag{31}$$

The above equation is backward. If $\lambda^I_{i,j}$ is given, the Lagrange multiplier can be updated iteratively through the above equation.

At any time t, for any pair of source node i and destination node j, the following equation can be obtained by seeking the solution of $\frac{\partial L_d}{\partial p^t_{i,j}} = 0$,

$$\begin{aligned}m^t_{i,j}\frac{\partial c^t_{i,j}}{\partial p^t_{i,j}} &- \lambda^t_{i,j}\frac{m^t_{i+1,j}-m^t_{i-1,j}}{2\delta_e} \\ &+ \frac{\partial a^t_{i,j}}{\partial p^t_{i,j}}\lambda^t_{i,j}\frac{m^t_{i,j+1}-m^t_{i,j-1}}{2\delta_\mu} \\ &- \frac{\sigma_e^2}{2}\lambda^t_{i,j}\frac{m^t_{i+2,j}-2m^t_{i,j}+m^t_{i-2,j}}{4\delta_e^2} = 0.\end{aligned} \tag{32}$$

Our model is a convex game model, combined with convex programming theory to ensure that the problem model is a convex problem. So, the equilibrium solution must exist and is the optimal solution.

According to the above formula, the mean field $m^{t+1}_{i,j}$, Lagrangian parameter$\lambda^{t-1}_{i,j}$ and power level $p^t_{i,j}$ can be iteratively updated to obtain the optimal power value. The power control algorithm is designed as shown in Algorithm 1 and the symbols and notations used in the above derivation are summarized in Table III.

B. Frequency Scheduling and Relay Selection

In Algorithm 1, given the link information (i, j), frequency f, and time information $[0, T]$, it is necessary to initialize the mean field distribution $m^0_{:,:}$, Lagrange multiplier $\lambda^I_{:,:}$, and power level $p^0_{:,:}$, and iteratively update the mean field, Lagrange multiplier, and power in the time axis X, energy state space Y, and interference state space Z. Mean field is obtained by solving FPK equation, and value function is obtained by solving HJB equation. When the algorithm reaches the convergence condition, the optimal power control strategy $p^*_{i,j}(f)$ can be obtained.

The frequency scheduling algorithm needs to maximize the utility function $c^f_{i,j}$. Since the optimized value of the utility function in power has been solved by Algorithm 1. The maximized value of which can be obtained by traversing the available frequency f over a given link. Therefore, the frequency scheduling algorithm can be designed as shown in Algorithm 2. First of all, we give the link information (i, j) and initialize f^* and $c^*_{i,j}$ to 0. Then, it calculates the utility function by traversing the frequencies at the available frequencies. By comparing the utility function, the optimal frequency f^* and the maximized value $c^*_{i,j}$ can be obtained.

The relay selection needs to consider the cost function of the link $T^f_{i,j}$. The smaller cost in a link, the better performance and stability of information transmission. When minimizing the cost function, the link utility function $c^f_{i,j}$ can be obtained by the frequency scheduling algorithm, and the packet queue length and relative speed can be calculated locally. Therefore, the relay selection algorithm can be designed as shown in Algorithm 3. It calculates the cost function of all next hop nodes in $next(i)$ which node i can be reached, by comparing the value of the cost function, node j^* corresponding to the optimal link quality is obtained. Then, the data in node i will be transmitted to it.

In summary, the cross-layer resource management algorithm

Algorithm 1 Power control algorithm

Input: The link information (i, j), frequency f, and time information $[0, T]$, time dispersion X, energy state dispersion Y, and interference state dispersion Z
Initialize the mean field distribution $m^0_{:,:}$, Lagrange multiplier $\lambda^I_{:,:}$, and power level $p^0_{:,:}$
While the convergence condition of the algorithm
/*Update the mean field, Lagrange multiplier, and power in the time axis X, energy state space Y, and interference state space Z iteratively*/
  For $t = 1 : 1 : X + 1$ **do**
    For $i = 1 : 1 : Y + 1$ **do**
      For $j = 1 : 1 : Z + 1$ **do**
        Update mean field:
        $m^{t+1}_{i,j}$ using (28).
        Update Lagrangian parameter:
        $\lambda^{t-1}_{i,j}$ using (31).
        Update power levels:
        $p^t_{i,j}$ using (32).
      END
    END
  END
END
Output: The optimal power control strategy $p^*{}_{i,j}(f)$

Algorithm 2 Frequency scheduling algorithm

Input: The link information (i, j)
Initialize f^* and $c^*_{i,j}$ equal to 0
/* Obtain the maximized value of $c^*_{i,j}$ by traversing the available frequency f over a given link (i, j)*/
For $k = 0$; $k <$ max − min; $k + +$ **do**
  Given (i, j) and $f_{\max+k}$, obtain ${c_{i,j}}^{f_{\min+k}}$ by calling Algorithm 1
  If ${c_{i,j}}^{f_{\min+k}} > c^*_{i,j}$
    $c^*_{i,j} = {c_{i,j}}^{f_{\min+k}}$
    $f^* = f_{\min+k}$
  END
END
Output: The optimal frequency f^* and the maximized value of $c^*_{i,j}$

Algorithm 3 Relay selection algorithm

Input: Node i and the next hop set $next(i)$ of node i
  Initialize j^* is NULL
  /*Obtain the optimal relay node j^* by minimizing the cost in link $(i, next\,(i))$*/
While $j \in next(i)! =$NULL
  Obtain $c_{i,j}^*$ by calling Algorithm 2 and compute $T_{i,j}^*$
  If $T_{i,j}^* < T^*$
    $T^* = T_{i,j}{}^*$
    $j^* = j$
  END
  $j = j \rightarrow next$
END
Output: The optimal relay node j^* and its corresponding cost $T_{i,j}^*$

consists of three parts as shown in Fig. 3 with a power control algorithm, a frequency scheduling algorithm, and a relay selection algorithm. The relay selection algorithm completes the selection of the relay node by calling the power control algorithm and the frequency scheduling algorithm. Correspondingly, the power control algorithm and the frequency scheduling algorithm provide services for the relay selection algorithm. These three algorithms are used together to solve the cross-layer resource management problem in swarm FANET.

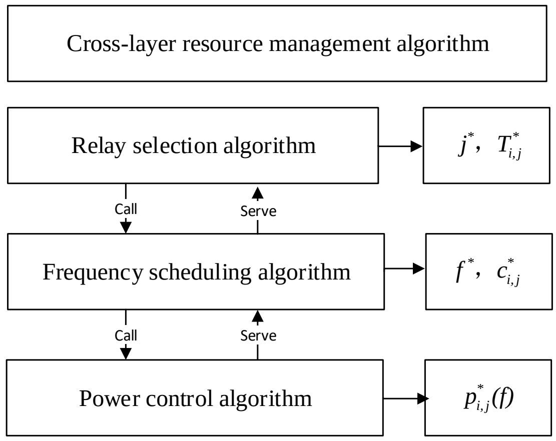

Fig. 3. Cross-layer resource management algorithm.

Routing request ID	Source node ID	Destination node ID	Hop count	Time to live	Path cache record

(a) Routing request packet

Routing response ID	Source node ID	Destination node ID	Hop count	Time to live	**Link quality**	Path record

(b) Routing response packet

Fig. 4. Routing packet format in CLRM-DSR.

C. CLRM-DSR Protocol

The DSR protocol is a typical MANET routing protocol [7]. This protocol does not need to broadcast routing information periodically to maintain routing tables, the routing overhead in the DSR protocol is less than that in the OLSR and other routing protocols [45]. As two mechanisms of DSR, route lookup and route maintenance ensure that every node can construct an available route in the network. However, since there is a route lookup process before the packet is sent, the end-to-end delay in the DSR increases. More importantly, the nodes in the DSR protocol don't exchange link quality information. When the network topology and links change, the performance of the FANET network using the DSR protocol is unstable, especially in terms of data packet transmission rate [51].

In the FANET, the nodes move at a high speed so that the routing information found by using the DSR protocol is likely to expire [52]. The link quality between nodes can ensure the stability of the links and routing information when nodes are looking for routes. Therefore, as shown in Fig. 4, link quality is employed in the route response message, which refers to the optimal cost function obtained by the cross-layer resource management algorithm. To reduce the routing overhead, the format of the routing request message in the CLRM-DSR protocol leaves it as it is in the DSR protocol.

The CLRM-DSR routing protocol will send a request when there is a need for information transmission without periodically broadcasting routing information. When a node needs to send data, the source node finds whether the routing information of the destination node information exists locally, if it exists, the node can send the information directly, otherwise it needs to send a routing request packet 3(a) to perform the route discovery process to find the path to the destination node.

When the destination node receives a routing request packet, it sends a route response message in the unicast mode, the intermediate node calls the cross-layer resource management algorithm to obtain the link quality metric $T_{i,*}$. The link quality field in the packet will be replaced by the new value after adding $T_{i,*}$. When the source node receives the route response packet, it can obtain the link quality metric to other nodes $T_{i,*}$. Since on the transmission path, $T_{i,*}$ is updated according to the state of the link, the link corresponding to the smallest $T_{i,*}$ obtained at the source node is the most stable link, which is the optimal link for data transmission.

V. EXPERIMENTS AND RESULTS

In this paper, the CLRM-DSR protocol based on the proposed cross-layer resource management algorithm is simulated and compared with the conventional DSR protocol. A specific FANET scenario is considered which is formed by UAVs in a space of $3\ km * 3\ km * 3\ km$, and the number of UAVs ranges from 10 to 60, of which 3–18 nodes send constant bit rate (CBR) to the corresponding destination nodes [42]. To reach the equilibrium state quickly, the initial power is set to half of the maximum power. Ultra-dense deployment and

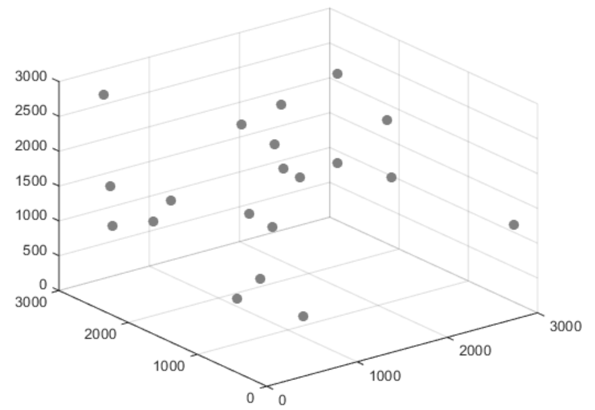

Fig. 5. Simulation node spatial distribution scenario.

TABLE IV
SIMULATION PARAMETERS.

Parameter	Value
Simulation space	3 km * 3 km * 3 km
UAV quantity	10–60
UAV speed (m/s)	60–100
Communication radius (m)	1000
Frequency band (GHz)	2.4
Channel bandwidth (MHz)	20
Bit rate (Mbps)	1
Coding rate	0.5
Node maximum energy (J)	6
Maximum power (w)	0.2
Time dispersion X	50
Energy state dispersion Y	10
Interference state dispersion Z	10
Application layer service	CBR
Packet size (Byte)	512
Time interval (ms)	1

three-dimensional distribution are the characteristics of ultra-dense FANET driven by UAV clusters. In the simulation, the FANET simulation scenario with node spatial distribution is adopted as shown in Fig. 5. Detailed simulation parameters are listed in Table IV.

To demonstrate the performance of the algorithm, the packet delivery rate, end-to-end delay, and routing overhead are mainly considered. The performance of the CLRM-DSR and conventional DSR protocol are compared by different speeds and numbers of UAVs based on the statistics, which are shown separately in Section V-B.

A. Simulation Platform

In this paper, a FANET simulation platform is built. In this platform, the object-oriented method is used to model nodes in MATLAB. As shown in Fig. 6, the node model contains node-related attribute parameters, node movement model module, a complete protocol stack, data packet receiving and sending module, and information statistics module. Nodes interact through event response or command to simulate the operation of the FANET. This node model can complete simulation tests, including the interface of network layer routing protocol, MAC layer access protocol interface, MAC layer frequency scheduling, and physical layer power control.

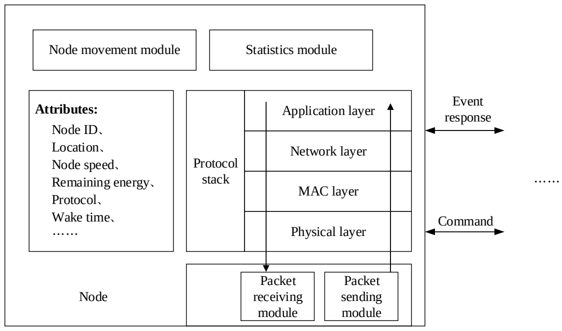

Fig. 6. Node model in simulation platform.

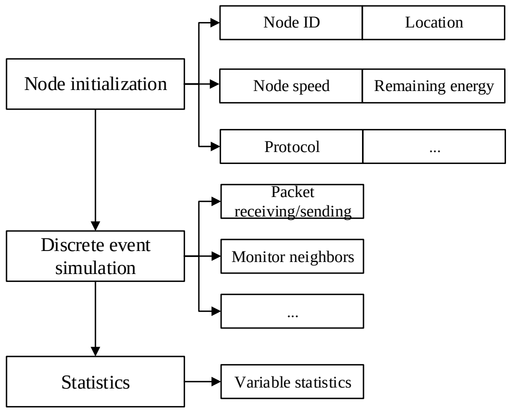

Fig. 7. Running process of the simulation platform.

1) Network layer routing protocol interface: The routing protocol is one of the critical issues of the FANET, which has a significant impact on network stability and performance [53]. Thus, the simulation platform provides a unified routing protocol initialization interface in the network layer, which can support the development and performance verification of various routing protocols.

2) MAC layer access protocol interface: The MAC layer access protocol is another essential issue in the FANET. Like the routing protocol interface, the simulation platform provides a unified initialization interface of MAC layer access protocol, which can support the development and performance verification of various MAC layer access protocols.

3) MAC layer frequency scheduling: The frequency resources of UAVs are limited. It is essential to schedule the frequency resources properly and improve resources utilization to achieve better network performance. The simulation platform builds a complete FANET environment. Based on this platform, the MAC scheduling scheme can be implemented, and the performance can be verified.

4) Physical layer power control: As UAVs become miniaturized, intelligent, and clustered, which makes the problem of energy limitation more prominent. It is necessary to design an efficient power control algorithm to improve energy utilization efficiency. In this simulation platform, the performance of the proposed power control algorithm can be verified.

Fig. 7 demonstrates the running process of the simulation platform. The platform will complete the parameters configuration of the FANET, after it is started. Subsequently, the discrete event simulation process completes the simulation of the FANET operation by simulating the processing of services in the network, including the packet receiving process, packet sending process, etc. Finally, the statistics process completesThe statistics process completes the statistics of network performance indicators, which is convenient for evaluating the proposed algorithm.

In this paper, the proposed cross-layer resource management algorithm and the CLRM-DSR protocol in FANET are verified in this platform. Meanwhile, this simulation platform can also implement the algorithm verification of the conventional mobile ad-hoc network and the vehicle network.

B. Simulation Results

In the actual simulation, all nodes are traversed in a simulation interval to achieve the purpose of processing the data services of all network nodes. Furthermore, more stable indicators statistics of performance are achieved through traversal many times.

1) Performance of CLRM-DSR and DSR protocol about different speeds of UAVs: In this section, the impact of UAV speeds on the performance of two routing protocols is analyzed. In this scenario, the number of UAVs is 30, the number of communication node pairs is 8. The packet delivery rate, end-to-end delay, and routing overhead under different UAV speeds (60 m/s, 70 m/s, 80 m/s, 90 m/s, and 100 m/s [3]) are shown in Fig. 8.

Fig. 8(a) shows the packet delivery rate of the DSR and the CLRM-DSR protocol with different speeds of UAVs. As illustrated in Fig. 8(a), the packet delivery rate of both protocols shows a downward trend with the increasing speeds of UAVs. When the speed of UAVs is 60 m/s, the difference between the packet delivery rate of the CLRM-DSR and the DSR protocol is 3%. However, when the speed of UAVs is 100 m/s, the difference is 6%. As the speed of UAVs increases, the change of network topology is intensified, and the communication links between the nodes are broken, which will lead to a decrease in packet delivery rate. UAVs have a wide range of speed variations in practical applications. The CLRM-DSR protocol performs better packet delivery rate performance than the DSR protocol as shown in Fig. 8(a). The main reason is that the CLRM-DSR protocol introduces the results of cross-layer resource management policy and uses link quality to select stable links, which reduces repeated routing request packets caused by frequent breaking links. In general, CLRM-DSR weakens the impact of UAVs speeds on the packet delivery rate and improves the packet delivery rate.

Fig. 8(b) indicates the end-to-end delay of the DSR and the CLRM-DSR protocol with different UAVs speeds. As illustrated in Fig. 8(b), the end-to-end delay of both protocols shows an upward trend with the increasing speeds of UAVs. When the speed of UAVs is 60 m/s, the difference between the end-to-end delay of the CLRM-DSR and the DSR protocol is 210 ms. However, when the speed of UAVs is 100 m/s, the difference is 280 ms. The UAV with high mobility causes drastic changes in the network topology, and results in unstable links, which makes the DSR protocol cache or even the newly created routing information outdated. The possibility of data retransmission will increase. To correctly transmit data, the route search process needs to be reinitialized, and the time it takes by finding routes frequently increases the end-to-end delay. However, the CLRM-DSR protocol selects stable paths based on link quality, which reduces the probability of route

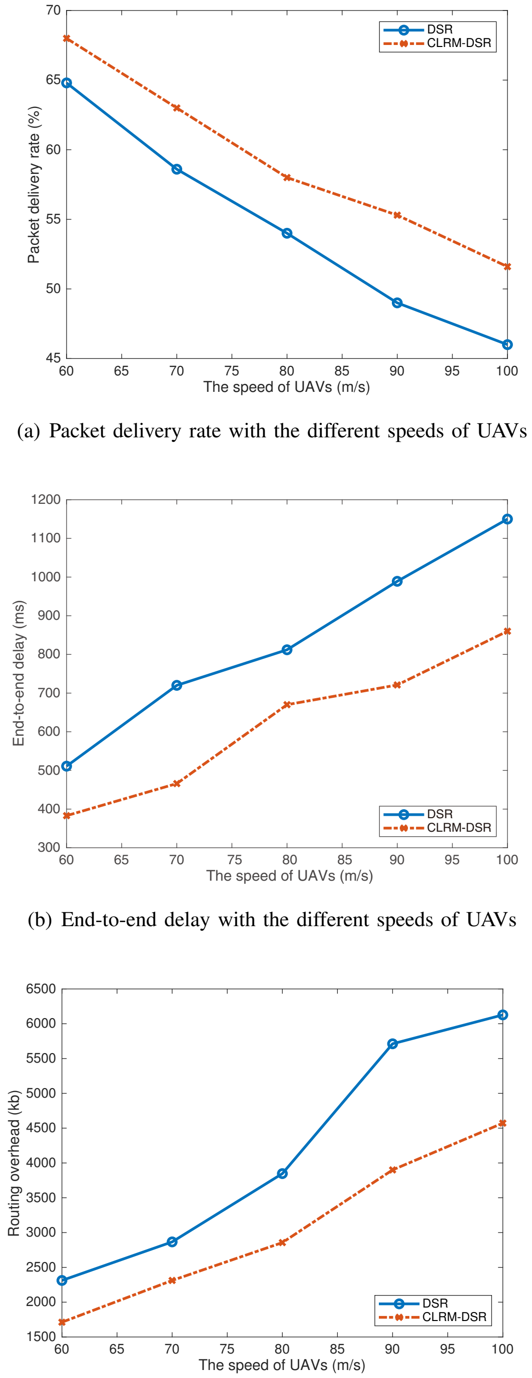

(a) Packet delivery rate with the different speeds of UAVs

(b) End-to-end delay with the different speeds of UAVs

(c) Routing overhead with the different speeds of UAVs

Fig. 8. Network performance about different speeds of UAVs.

errors and the extra delay caused by the route lookup process. In general, the end-to-end delay in the CLRM-DSR protocol is lower than that in the DSR protocol, which weakens the impact of UAV speeds on the end-to-end delay and reduces the end-to-end delay.

Fig. 8(c) depicts the routing overhead of the DSR and the CLRM-DSR protocol with different UAVs speeds. As shown in Fig. 8(c), the routing overhead of both protocols shows an upward trend with the increasing speeds of UAVs. When the speed of UAVs is 60 m/s, the difference between the routing overhead of the CLRM-DSR and the DSR protocol is 600 kb. However, when the speed of UAVs is 100 m/s, the difference is 1600 kb. With the increase of UAVs speed, the frequently broken links lead to a large amount of wrong routing information. As a typical on-demand routing protocol, when the data need to be transmitted, the route lookup process in the DSR protocol should be reinitialized. This process brings several control packets, including routing request packets and routing reply packets, which results in a sharp increase in routing overhead. Limited by the network capacity, the routing overhead will tend to be flat at last. Since the CLRM-DSR protocol reduces the impact of node mobility on the communication path by link quality, the number of control packets transmitted in the network is reduced. Therefore, the CLRM-DSR protocol is more effective than DSR protocol in routing overhead, which weakens the impact of UAVs speeds on the routing overhead and reduces the routing overhead.

2) Performance of CLRM-DSR and DSR with different numbers of UAVs: This section mainly analyzes the impact of UAV numbers on the performance of the two routing protocols. In this scenario, the UAVs move at a speed of 100 m/s. The packet delivery rate, end-to-end delay, and routing overhead under the different numbers of UAVs (10, 20, 30, 40, and 50) are demonstrated in Fig. 9.

Fig. 9(a) shows the packet delivery rate of the DSR protocol and the CLRM-DSR protocol with different numbers of UAVs. The UAVs are sparsely distributed, when the number of UAVs is relatively small. In this scenario, the path between nodes is few or even doesn't exist. At this time, the performance is no difference between the CLRM-DSR protocol and the DSR protocol. Therefore, when the number of UAVs is 10, the delivery rates of the two protocols are the same. The connectivity probability between UAVs increases with the increasing number of UAVs. The UAV with CLRM-DSR protocol selects the path according to the link quality, which ensured that the selected link is more stable than that selected by DSR. Thus, it can achieve better performance than the conventional DSR protocol in the packet delivery rate. For the DSR protocol, when the number of UAVs increases, the interference and collisions in the network become more serious. For instance, when the number of UAVs exceeds 20, the packet delivery rate decreases significantly. For the CLRM-DSR protocol, when the number of UAVs is not particularly large, the performance gain brought by the presented protocol is greater than the impact of the increase in network scale.

Fig. 9(b) depicts the end-to-end delay of the DSR protocol and the CLRM-DSR protocol with different numbers of UAVs. When the number of UAVs is less, some nodes in the network

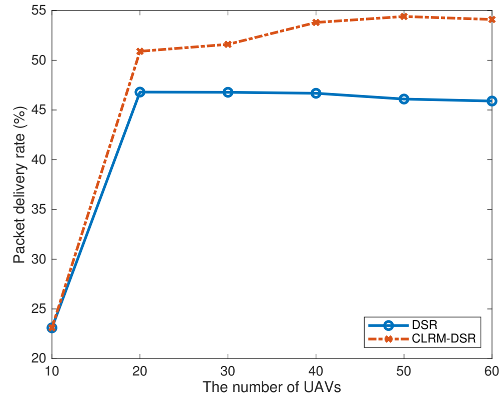

(a) Packet delivery rate with the different numbers of UAVs

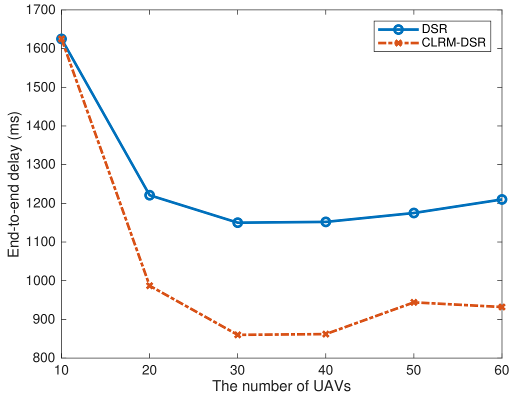

(b) End-to-end delay with the different numbers of UAVs

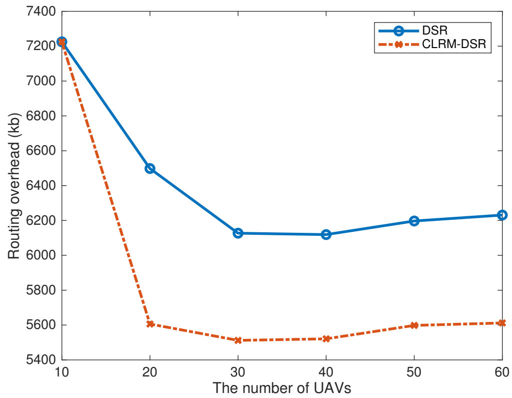

(c) Routing overhead with the different numbers of UAVs

Fig. 9. Network performance with regard to different numbers of UAVs.

may be unconnected or have only one available path. In order to send data, a lot of routing overhead is generated in the network. Thus, communication under two routing protocols has a high end-to-end delay. Overall, the CLRM-DSR protocol has an advantage over the DSR in end-to-end delay. It is because that the number of paths between UAVs increases as the number of UAVs increases. For the DSR protocol, it needs to continually re-route because of the frequently disconnected communication links. The CLRM-DSR protocol can alleviate the frequent disconnection of connections and avoid the extra delay caused by re-routing. When the number of UAVs exceeds 40, the interference and conflicts in the system are severe, and the delay of both protocols will increase.

Fig. 9(c) illustrates the routing overhead of the DSR protocol and the CLRM-DSR protocol with different numbers of UAVs. When the number of UAVs is too less, the links between the UAVs are unstable. The source UAVs need to continuously perform the routing request process to send data, which leads to a large amount of routing overhead. With the increasing number of UAVs, the number of routing request packets is reduced. However, the UAVs still need to continually find the right routes due to the frequently disconnected communication links. Result from the mechanism of routing based on link quality, the selected path can be more robust in the CLRM-DSR protocol. The network with the CLRM-DSR protocol will lead to less routing overhead than the DSR protocol.

Through the simulation comparison of CLRM-DSR and DSR in the designed simulation platform, a conclusion can be obtained that the CLRM-DSR protocol has improved compared with the conventional DSR protocol in packet delivery rate, end-to-end delay, and routing overhead. Besides, the cross-layer resource management algorithm using the MFG has a gain effect in swarm UAV communications.

VI. CONCLUSION

In the paper, we study the cross-layer design method and MFG theory in large-scale FANET. The cross-layer design method breaks the communication limitations between layers. Each layer can share local information through inter-layer interaction, which can effectively improve the efficiency of resource utilization of FANET. The MFG provides a feasible analysis, modeling and solution method for large-scale network power control. We jointly consider physical layer power resources, MAC layer frequency resources, and network layer routing resources, and proposes a cross-layer resource management method. Meanwhile, we present a routing protocol named CLRM-DSR based on cross-layer optimization with MFG for multi-hop swarm UAV networks, which adds link quality measurement. The simulation results prove the advantage of CLRM-DSR used MFG in swarm UAV networks. Last but not least, the paper studies the homogeneous network communication scenario composed of UAVs. Under the requirements of the future space-air-ground integrated networking, various networks will coordinate with each other to complete tasks, and the network performance of the proposed algorithm applied in heterogeneous networks is unknown. The study of cross-layer design and the application of MFG in different routing protocols of a heterogeneous network is one of our future works. At the same time, MAC layer protocol design, path planning, node rate control, congestion control, and other aspects also have a great impact on FANET. For further research, we intend to study the above issues in depth.

REFERENCES

[1] M. E. Mkiramweni, C. Yang, J. Li, and Z. Han, "Game-theoretic approaches for wireless communications with unmanned aerial vehicles," *IEEE Wireless Commun.*, vol. 25, no. 6, pp. 104–112, Dec. 2018.

[2] Z. Han, A. Swindlehurst, and K. Liu, "Smart deployment/movement of unmanned air vehicle to improve connectivity in MANET," in *Proc. IEEE WCNC*, 2006, pp. 252–257.

[3] M. Khan, A. Safi, I. Qureshi, and I. Khan, "Flying ad-hoc networks (FANETs): A review of communication architectures, and routing protocols," in *Proc. INTELLECT*, 2017, pp. 1–9.

[4] A. Vengadesh and P. Gunasekaran, "Design and development of aircraft to aircraft communication by ad-hoc networks," in *Proc. ICCPCT*, 2015.

[5] M. Erdelj, E. Natalizio, K. Chowdhury, and I. Akyildiz, "Help from the sky: Leveraging UAVs for disaster management," *IEEE Pervasive Comput.*, vol. 16, no. 1, pp. 24–32, Mar. 2017.

[6] I. Khan *et al.*, "RSSI-controlled long-range communication in secured IoT-enabled unmanned aerial vehicles," *Mob. Inf. Syst*. vol. 2021, pp. 1–11, Mar. 2021.

[7] I. Bekmezci, O. Sahingoz, and S. Temel, "Flying ad-hoc networks (FANETs): A survey," *AD Hoc Netw.*, vol. 11, no. 3, pp. 1254–1270, May 2013.

[8] Y. Zeng, R. Zhang, and T. Lim, "Wireless communications with unmanned aerial vehicles: Opportunities and challenges," *IEEE Commun. Mag.*, vol. 54, no. 5, pp. 36–42, May 2016.

[9] O. K. Sanhingoz, "Networking models in flying ad-hoc networks (FANETs): Concepts and challenges," *J. Intell. Robot. Syst.*, vol. 74, no. 1, pp. 513–527, Apr. 2014.

[10] L. Tan, Z. Zhu, F. Ge, and N. Xiong, "Utility maximization resource allocation in wireless networks: Methods and algorithms," *IEEE Trans. Syst. Man. Cybern.: Syst.*, vol. 45, no. 7, pp. 1018–1034, Jul. 2015.

[11] T. Dapper e Silva, C. F. Emygdio de Melo, P. Cumino, D. Rosário, E. Cerqueira, and E. Pignaton de Freitas, "STFANET: SDN-based topology management for flying ad hoc network," *IEEE Access*, vol. 7, pp. 173499–173514, Nov. 2019.

[12] J. Zander and S. Kim, *Radio resource management for wireless networks*, Boston, Artech House, 2001.

[13] V. Srivastava and M. Motani, "Cross-layer design: A survey and the road ahead," *IEEE Commun. Mag.*, vol. 43, no. 12, pp. 112–119, Dec. 2005.

[14] J. Peng, H. Niu, and W. Huang, "Cross layer design and optimization for multi-hop ad hoc networks," in *Proc. IEEE IAEAC*, 2017, pp. 1678–1682.

[15] L. Le and E. Hossain, "Cross-layer optimization frameworks for multi-hop wireless networks using cooperative diversity," *IEEE Trans. Wireless Commun.*, vol. 6, no. 7, pp. 2592–2602, Jul. 2008.

[16] E. Setton, T. Yoo, and X. Zhu, "Cross-layer design of ad hoc networks for real-time video streaming," *IEEE Wireless Commun.*, vol. 12, no. 4, pp. 59–65, Aug. 2005.

[17] W. Yuen, H. Lee, and T. Andersen, "A simple and effective cross layer networking system for mobile ad hoc networks," in *Proc. IEEE PIMRC*, 2002, pp. 1952–1956.

[18] J. Peng, H. Niu, W. Huang, X. Yin, and Y. Jiang, "Cross layer design and optimization for multi-hop ad hoc networks," in *Proc. IEEE IAEAC*, 2017, pp. 1678–1682.

[19] Z. Han, D. Niyato, W. Saad, T. Basar, and A. Hjorungnes, *Game theory in wireless and communication networks: Theory, models and applications*, Cambridge University Press, UK, 2011.

[20] P. Li and H. Duan, "A potential game approach to multiple UAV cooperative search and surveillance," *Aerospace Sci. Technol.*, vol. 68, pp. 403–415, Sep. 2017.

[21] L. Ruan, J. Wang, and J. Chen, "Energy-efficient multi-UAV coverage deployment in UAV networks: A game-theoretic framework," *China Commun.*, vol. 15, no. 10, pp. 194–209, Oct. 2018.

[22] P. Charlesworth, "Using non-cooperative games to coordinate communications UAV," in *Proc. GLOBECOM Workshop*, 2014, pp. 1463–1468.

[23] M. E. Mkiramweni, C. Yang, J. Li, and W. Zhang, "A survey of game theory in unmanned aerial vehicles communications," *IEEE Commun. Surveys Tuts.*, vol. 21, no. 4, pp. 3386–3416, May 2019.

[24] C. Yang, H. Dai, J. Li, Y. Zhang and Z. Han, "Distributed interference-aware power control in ultra-dense small cell networks: A robust mean field game," *IEEE Access*, vol. 6, pp. 12608–12619, Jan. 2018.

[25] A. Al-Zahrani, F. Yu, and M. Huang, "A joint cross-layer and colayer interference management scheme in hyperdense heterogeneous networks using mean-field game theory," *IEEE Trans. Veh. Technol.*, vol. 65, no. 3, pp. 1522–1535, Mar. 2016.

[26] C. Yang, J. Li, P. Semasinghe, E. Hossain, S. Perlaza, and Z. Han, "Distributed interference and energy-aware power control for ultra-dense D2D networks: A mean field game," *IEEE Trans. Wireless Commun.*, vol. 16, no. 2, pp. 1205–1217, Dec. 2017.

[27] P. Semasinghe and E. Hossain, "Downlink power control in self-organizing dense small cells underlaying macrocells: A mean field game," *IEEE Trans. Mobile Comput.*, vol. 15, no. 2, pp. 350–363, Mar. 2016.

[28] Z. Han, D. Niyato, W. Saad, and T. Basar, *Game theory for next-generation wireless and communication networks: Modeling, analysis, and design*, Cambridge University Press, UK, 2019.

[29] S. Raj, V. Panchal, P. Vashist, and R. Chopra, "FANETs: Current trends and challenges," in *Proc. IEEE PEEIC*, 2019, pp. 472–475.

[30] S. Maakar, Y. Singh, and R. Singh, "Flying ad hoc network: A newest research area for ad hoc networks," in *Proc. IEEE ICCT*, 2019, pp. 298–302.

[31] O. Oubbati, M. Atiquzzaman, P. Lorenz, M. Tareque, and M. S. Hossain, "Routing in flying ad hoc networks: Survey, constraints, and future challenge perspectives," *IEEE Access*, vol. 7, pp. 81057–81105, 2019.

[32] P. Xie, "An enhanced Olsr routing protocol based on node link expiration time and residual energy in ocean FANETS," in *Proc. APCC*, 2018, pp. 598–603.

[33] X. Fan, J. Lin, C. Zhang, and S. Zhang, "A cross-layer antijamming routing protocol for FANETS," in *Proc. IEEE ICCC*, 2018, pp. 301–305.

[34] I. Khan, I. M. Qureshi, M. A. Aziz, T. A. S. Cheema, and S. B. Hussain,"Smart IoT control-based nature inspired energy efficient routing protocol for flying ad hoc network (FANET)," *IEEE Access*, vol. 8, pp. 56371–56378, Mar. 2020.

[35] S. Nath, I. Das, S. Roy, A. Jana, J. Sing, and S. Sarkar, "Enhancing packet delivery rate in flying ad-hoc network (FANET) routing," in *Proc. IEEE R10 HTC*, 2019, pp. 66–70.

[36] I. Mahmud and Y. Cho, "Adaptive hello interval in FANET routing protocols for green UAVs," *IEEE Access*, vol. 7, pp. 63004–63015, May 2019.

[37] B. Bellur, M. Lewis, and F. Templin, "An ad-hoc network for teams of autonomous vehicles," in *Proc. AINS*, 2002, pp. 1–6.

[38] B. Bellur and R.Ogier, "A reliable efficient topology broadcast protocol for dynamic networks," *IEEE Comput. Commun. Soc.*, vol. 1, no. 2, pp. 178–186, Mar. 1999.

[39] T. Brown, S. Doshi, S. Jadhav, and D. Henkel, "A full scale wireless ad hoc network test bed," in *Proc. ISART*, 2005, pp. 50–60.

[40] V. Khare, F. Wang, and S. Wu, "Ad-hoc network of unmanned aerial vehicle swarms for search & destroy tasks," in *Proc. IEEE IS*, 2008, pp. 65–72.

[41] M. Khan, I. Khan, A. Safi, and I. Quershi, "Dynamic routing in flying ad-hoc networks using topology-based routing protocols," *Drones*, vol. 2, no. 3, pp. 27–42, Aug. 2018.

[42] S. Al-Emadi and A. Al-Mohannadi, "Towards enhancement of network communication architectures and routing protocols for FANETs: A survey," in *Proc. IEEE CommNet*, 2020, pp. 1–10.

[43] A. Leonov, G. Litvinov, and D. Korneev, "Simulation and analysis of transmission range effect on AODV and OLSR routing protocols in flying ad hoc networks (FANETs) formed by mini-UAVs with different node density," in *Proc. SYNCHROINFO*, 2018, pp. 1–7.

[44] A. Garcia-Santiago, J. Castaneda-Camacho, J. F. GuerreroCastellanos, and G. Mino-Aguilar, "Evaluation of AODV and DSDV routing protocols for a FANET: Further results towards robotic vehicle networks," in *Proc. IEEE LASCAS*, 2018, pp. 1–4.

[45] A. Sharma and R. Kumar, "Performance comparison and detailed study of AODV, DSDV, DSR, TORA and OLSR routing protocols in ad hoc networks," in *Proc. PDGC*, 2016, pp. 732–736.

[46] M. Y. Arafat and S. Moh, "Routing protocols for unmanned aerial vehicle networks: A survey," *IEEE Access*, vol. 7, pp. 99694–99720, Jul. 2019.

[47] G. Tan, Q. Zhang, L. Zhang, and Y. Li, "Characterizing the interference distribution in MANETs with different mobile models," in *Proc. IEEE ITNEC*, 2016, pp. 141–144.

[48] T. Alpcan *et al.*, "Mechanisms and games for dynamic spectrum allocation," *Cambrige University Press* , 2013.

[49] Y. Zhang, C. Yang, J. Li, and Z. Han, "Distributed interference-aware traffic offloading and power control in ultra-dense networks: Mean field game with dominating player," *IEEE Trans. Veh. Technol.*, vol. 68, no. 9, pp. 8814–8826, Sep. 2019.

[50] Mean field games. [Online] Available: https://terrytao.wordpress.com/2010/01/07/mean-field-equations.

[51] A. Barve, A. Kini, O. Ekbote, and J. Abraham, "Optimization of DSR routing protocol in MANET using passive clustering," in *Proc. IEEE CCIS*, 2016, pp. 23–27.

[52] A. Nayyar, "Flying adhoc network (FANETs): Simulation based performance comparison of routing protocols: AODV, DSDV, DSR, OLSR, AOMDV and HWMP," in *Proc. icABCD*, 2018, pp. 1–9.

[53] L. Gupta, R. Jain, and G. Vaszkun, "Survey of important issues in UAV communication networks," *IEEE Commun. Surveys Tuts.*, vol. 18, no. 2, pp. 1123–1152, Sep. 2016.

TONG LI received the bachelor's degree in Electronic Information Engineering, in 2020 from Chang'an University, Xi'an, China, where she is currently working toward the doctoral degree in information and communication engineering. She is also with the GUIDE Research Team, under the guidance of Dr. C. Yang. Her research interests include wireless ad hoc network and communication protocol.

CONG LI received his doctoral degree at Xidian university, Xi'an, China, in 2018. He works as an engineer at Academy of Space Electronic Information Technology, Xi'an, where he leads the research team of "intelligent satellite system". He has published one book on machine learning and more than 10 journals and conferences. His research interests are intelligent satellite communications, software-defined multi-function satellite payloads, and so on.

CHUNGANG YANG (S'09, M'11, SM'19) is a Full Professor at Xidian University, where he leads the research team of "GUIDE, Game, Utility, artificial Intelligent Design for Emerging communications". He has edited two books, and published 30 journals and 30 conferences. His research interests are artificial intelligent 6G wireless mobile networks, intent-driven networks (IDN), space-terrestrial networks (STN), and game theory for emerging communication networks.

JUNQI SHAO received the bachelor's degree in Network Engineering in 2018 from North China University of Water Resources and Electric Power, Zhengzhou, China, where he is currently working toward the master's degree in Information and Communication Engineering. He is also with the GUIDE Research Team, under the guidance of Dr. C. Yang. His research interests include wireless ad hoc network and communication protocol.

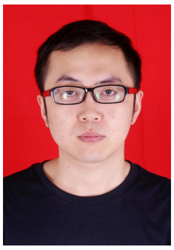

YUE ZHANG received the bachelor's degree in Communication Engineering from Xidian University in 2012, where he is currently working toward the M.S. degree. He is with the research team of "GUIDE, Game, Utility, artificial Intelligent Design for Emerging communications," which is guided by Dr. C. Yang. His research interests include crosslayer design for ad hoc networks and mean field game with dominators.

LEI PANG received the bachelor's degree in Communication Engineering from Xidian University, Xi'an, China, in 2018. Since 2018, he has been working toward the master degree in Electronic and Communication Engineering at Xidian University. He is currently with the GUIDE Research Team, which is guided by Dr. Chungang Yang. His research interests include intent-driven network (IDN) and wireless software defined network (SDN).

LIZHONG CHANG received the bachelor's degree in Electronic Information Engineering, in 2018 from Guizhou University, Guizhou, China, where he is currently working toward the master's degree in Information and Communication Engineering. He is also with the GUIDE Research Team, under the guidance of Dr. C. Yang. His research interests include wireless ad hoc network and communication protocol.

LINGLI YANG received the bachelor's degree in Communication Engineering from Xidian University, Xi'an, China, in 2019. Since 2019, she has been working toward the master's degree in Information and Communication Engineering with Xidian University, Xi'an, China. She is currently with the GUIDE Research Team, which is guided by Dr. C. Yang. Her research interests include wireless ad hoc network and communication protocol.

ZHU HAN (S'01-M'04-SM'09-F'14) received the B.S. degree in Electronic Engineering from Tsinghua University, in 1997, and the M.S. and Ph.D. degrees in Electrical and Computer Engineering from the University of Maryland, College Park, in 1999 and 2003, respectively. From 2000 to 2002, he was an R&D Engineer of JDSU, Germantown, Maryland. From 2003 to 2006, he was a Research Associate at the University of Maryland. From 2006 to 2008, he was an Assistant Professor at Boise State University, Idaho. Currently, he is a John and Rebecca Moores Professor in the Electrical and Computer Engineering Department as well as in the Computer Science Department at the University of Houston, Texas. His research interests include wireless resource allocation and management, wireless communications and networking, game theory, big data analysis, security, and smart grid. Dr. Han received an NSF Career Award in 2010, the Fred W. Ellersick Prize of the IEEE Communication Society in 2011, the EURASIP Best Paper Award for the Journal on Advances in Signal Processing in 2015, IEEE Leonard G. Abraham Prize in the field of Communications Systems (best paper award in IEEE JSAC) in 2016, and several best paper awards in IEEE conferences. Dr. Han was an IEEE Communications Society Distinguished Lecturer from 2015- 2018, AAAS fellow since 2019 and ACM distinguished Member since 2019. Dr. Han is 1% highly cited researcher since 2017 according to Web of Science. Dr. Han is also the winner of 2021 IEEE Kiyo Tomiyasu Award, for outstanding early to mid-career contributions to technologies holding the promise of innovative applications, with the following citation: "for contributions to game theory and distributed management of autonomous communication networks."